Pharm Res (2011) 28:2848–2862
DOI 10.1007/s11095-011-0544-0

RESEARCH PAPER

Expression of GFP in the Mitochondrial Compartment Using DQAsome-Mediated Delivery of an Artificial Mini-mitochondrial Genome

Diana Lyrawati • Alan Trounson • David Cram

Received: 31 January 2011 / Accepted: 21 July 2011 / Published online: 11 August 2011

ABSTRACT

Purpose We describe a novel strategy for expression of GFP in mammalian mitochondria.

Methods The key components of the strategy were an artificially created mitochondrial genome pmtGFP and a DQAsome transfection system.

Results Using immunofluorescence and a combination of immunohistochemical and molecular based techniques, we show that DQAsomes are capable of delivering the pmtGFP construct to the mitochondrial compartment of the mouse macrophage cell line RAW264.7, albeit at low efficiency (1–5%), resulting in the expression of GFP mRNA and protein. Similar transfection efficiencies were also demonstrated in a range of other mammalian cell lines.

Conclusions The DQAsome-transfection technique was able to deliver the exogenous DNA into the cellular mitochondria and the pmtGFP was functional. Further optimization of this strategy would provide a flexible and rapid way to generate mutant cells and useful animal models of mitochondrial disease.

KEY WORDS DQAsome · GFP expression · mini-mitochondrial genome · mitochondrial gene delivery · transfection

A. Trounson
California Institute for Regenerative Medicine
San Francisco, California 94107, USA

D. Lyrawati • A. Trounson • D. Cram
Monash Immunology and Stem Cell Laboratories Monash University
Melbourne, Australia

Present Address:
D. Lyrawati (✉)
Laboratory of Pharmacy, Faculty of Medicine
Brawijaya University
Jl. Veteran
Malang, Indonesia
e-mail: eldi_7_98@yahoo.com

INTRODUCTION

The usefulness of gene targeting to manipulate the nuclear genome and alter gene expression has been widely recognized. However, development of techniques to genetically modify cellular mitochondria has been far more challenging. While many novel strategies and techniques have been employed to transfect DNA into mitochondria, including the use of glass beads (1), a gene gun (2,3), electroporation (4) and lipofection (5–8), none of these approaches has proved effective. More recently, mitochondrial delivery of chimeric DNAs conjugated to a mitochondrial targeting peptide has been demonstrated using electron microscopy (9–11), however, expression of these constructs was not verified. Other, attempts to transfect mitochondria using two different plasmid constructs containing the reporter genes ornithine transcarbamylase (12,13) and luciferase (14,15) designed for mitochondrial expression, has also been unsuccessful. The lack of success to date has largely been hampered by the unavailability of an efficient mitochondrial DNA delivery system.

More recently, liposome-like vesicles derived from dequalinium called DQAsomes have been shown to target and fuse with the mitochondrial membrane (16,17). To exploit the unique properties of DQAsomes, we have undertaken to design and construct an artificial mini-mitochondrial genome with the reporter green fluorescent protein (GFP) gene in an attempt to develop a novel mitochondrial transfection system. GFP from the jellyfish *Aequorea victoria* was specifically chosen as a reporter gene because its expression in the mitochondria can be easily monitored by fluorescence microscopy. In this paper, we report the successful development of a DQAsome based transfection protocol using the mini-mitochondrial construct pmtGFP and demonstrate GFP expression in the mitochondrial compartment.

MATERIALS AND METHODS

Oligonucleotides for Construction of mtgfp

Long oligonucleotides (80–100 nucleotides) for the construction of the mitochondrial *gfp* gene *(mtgfp)* were synthesized and PAGE purified by Biosearch Technologies, Inc, USA. Short oligonucleotides (18–22 nucleotides) for specific PCRs were synthesized and desalted by Pacific Oligos Pty Ltd, Australia. Oligonucleotide sequences used for the construction and characterization of the mini-mitochondrial construct pmtGFP are listed in Table I.

Generation of an Artificial Mitochondrial gfp Gene (mtgfp)

The pmtGFP construct was synthesized using a PCR-based strategy (Fig. 1). The GFP gene was divided into six fragments overlapping by 20–25 nucleotides where each fragment was created by two complementary oligonucleotides pairs (46–100 nucleotides) containing a modified sequence of the base substitutions necessary for correct codon usage and optimal expression in mammalian mitochondria (18,19). A linear mtgfp fragment of 717 bp was generated using two rounds of PCR. The first round involved 30 cycles of 30 s denaturation at 94°C and 30 s annealing-extension at 72°C in a standard PCR mixture containing 100 pmol each of long oligonucleotides: mtGF1, mtGR160, mtGF140, mtGR287, mtGF266, mtGR421, mtGF401, mtGR542, mtGF522, mtGR677, mtGF654 and mtGR726. A second round PCR was performed using 1% of the first round PCR product as a template with 10 pmol of short primers mtGF1s and mtGR726s, which were designed to anneal to the outermost ends of the fully extended mtgfp fragments. Standard thermal cycling conditions were used for second round PCR involving 30 cycles consisting of denaturation for 30 s at 94°C, annealing for 30 s at 56°C, and extension for 30 s at 72°C. The reaction mixture for first and second round PCRs contained 1x Taq PCR Buffer (50 mM KCl, 10 mM Tris–HCl, pH 9.0 and 1.5 mM $MgCl_2$) (Amersham Pharmacia Biotech, UK), 200 μM dNTPs, 0.2 μL Platinum Pfx DNA Polymerase and primers and DNA template as indicated. The ends of the mtgfp fragment were further modified using primers mtcL2664 and mtcH3424 (Table II) to generate the mtcGFP fragment for assembly into the pmtGFP construct.

Assembly of the Minimitichondrial Plasmid pmtGFP

The plasmid pmtGFP (5,896 bp) was assembled as a minimal mitochondrial genome consisting of pCR2.1 as the vector backbone (TA Cloning kit, Invitrogen) and three essential fragments of the mouse mini-mitochondrial genome (*mtc*) called mtO_H, mtO_L and mtcGFP. The mtO_H

Table I Oligonucleotides Used to Construct the mtgfp Fragment

Fragments	Primer code	Sequence 5′→3′[a]
Fragment 1 *mtgfp*	mtGF1 (99nt)	GAGGGTACCATGAGCAAAGGCGAAGAACTATTCACTGGCGTAGTCCCAATCCT CGTAGAACTAGATGGCGATGTAAAT***GGACACAAATTTTCTGTCAGC***
	mtGR160 (91nt)	***GGAGTTTTCCGGTGGTGCAG***ATTAATTTTAGGGTGAGTTTTCCGTATGTGGCA TCACCTTCACCTTCTCC***GCTGACAGAAAATTTGTGTCC***
Fragment 2 *mtgfp*	mtGF140 (99nt)	***CTGCACCACCGGAAAACTCC***CTGTACCATGACCAACACTAGTCACTACCCTAA CATACGGCGTACAATGCTTTTCCC***GATACCCAGACCATATGAAACA***
	mtGR287 (70nt)	***CGTTCTTGTACGTAGCCTTCGG***GCATGGCGCTTTTGAAAAAGTCATGT ***TGTTTCATATGGTCTGGGTATC***
Fragment 3 *mtgfp*	mtGF266 (89nt)	***CCGAAGGCTACGTACAAGAACG***AACCATCTTTTTCAAAGATGACGGAAACTAC AAAACCCGCGCTGAA***GTCAAATTCGAAGGTGACACC***
	mtGR421 (88nt)	***GTTTGTGGCCGAGGATGTTT***CCATCTTCTTTAAAGTCGATGCCTTTT AGTTCGATTCGATTTACAAG***GGTGTCACCTTCGAATTTGAC***
Fragment 4 *mtgfp*	mtGF401 (100nt)	***GAAACATCCTCGGCCACAAAC***TTGAATACAACTATAACTCCCACAATGTATACAT CATGGCAGACAAA***CAAAAAAATGGCATCAAAGTCAACTTCAAAAT***
	mtGR542 (74nt)	***TGGTCGGCTAGTTGTACGGAT***CCATCTTCGATGTTGTGTCGG ***ATTTTGAAGTTGACTTTGATGCCATTTTTTTG***
Fragment 5 *mtgfp*	mtGF522 (100nt)	***ATCCGTACAACTAGCCGACCA***TTATCAACAAAACACTCCAATCGGCGACGGCC CTGTACTACTCCCA***GACAACCATTACCTCTCCACCCAATCTGCCCTA***
	mtGR677 (89nt)	***GCGGTTACAAATTCAAGTAGGAC***CATGTGGTCTCGTTTTTCGTTGGGATCTTT AGA***TAGGGCAGATTGGGTGGAGAGGTAATGGTTGTC***
Fragment 6 *mtgfp*	mtGF654 (46nt)	***GTCCTACTTGAATTTGTAACCGC***TGCTGGAATCACACATGGCATGG
	mtGR726 (47nt)	CTCGGTACCCTATTTGTATAGTTCGT***CCATGCCATGTGTGATTCCAG***

[a] Sequences in bold italic indicates overlapping nucleotides between joining oligonucleotides

```
                1atgagcaaaggcgaagaactattcactggcgtagtcccaatcctcgtagaactagatggcgatgtaaatggacacaaattttct
Universal       M  S  K  G  E  E  L  F  T  G  V  V  P  I  L  V  E  L  D  G  D  V  N  G  H  K  F  S
Vertebrate      M  S  K  G  E  E  L  F  T  G  V  V  P  I  L  V  E  L  D  G  D  V  N  G  H  K  F  S
mitochondria

                gtcagcggagaaggtgaaggtgatgccacatacggaaaactcaccctaaaattaatctgcaccaccggaaaactccctgtacca
Universal       V  S  G  E  G  E  G  D  A  T  Y  G  K  L  T  L  K  L  I  C  T  T  G  K  L  P  V  P
Vertebrate      V  S  G  E  G  E  G  D  A  T  Y  G  K  L  T  L  K  L  I  C  T  T  G  K  L  P  V  P
mitochondria

             169tgaccaacactagtcactaccctaacatacggcgtacaatgcttttcccgatacccagaccatatgaaacaacatgacttttc
Universal       *
Vertebrate      W  P  T  L  V  T  T  L  T  Y  G  V  Q  C  F  S  R  Y  P  D  H  M  K  Q  H  D  F  F
mitochondria

Vertebrate      aaaagcgccatgcccgaaggctacgtacaagaacgaaccatctttttcaaagatgacggaaactGcaaaacccgcgctgaagtc
mitochondria    K  S  A  M  P  E  G  Y  V  Q  E  R  T  I  F  F  K  D  D  G  N  C  K  T  R  A  E  V

Vertebrate      aaattcgaaggtgacacccttgtaaatcgaatcgaactaaaaggcatcgactttaaagaagatggaaacatcctcggccacaaa
mitochondria    K  F  E  G  D  T  L  V  N  R  I  E  L  K  G  I  D  F  K  E  D  G  N  I  L  G  H  K

Vertebrate      cttgaatacaactataactcccacaatgtatacatcatggcagacaaacaaaaaaatggcatcaaagtcaacttcaaaatccga
mitochondria    L  E  Y  N  Y  N  S  H  N  V  Y  I  M  A  D  K  Q  K  N  G  I  K  V  N  F  K  I  R

Vertebrate      cacaacatcgaagatggatccgtacaactagccgaccattatcaacaaaacactccaatcggcgacggccctgtactactccca
mitochondria    H  N  I  E  D  G  S  V  Q  L  A  D  H  Y  Q  Q  N  T  P  I  G  D  G  P  V  L  L  P

Vertebrate      gacaaccattacctctccacccaatctgccctatctaaagatcccaacgaaaaacgagaccacatggtcctacttgaatttgta
mitochondria    D  N  H  Y  L  S  T  Q  S  A  L  S  K  D  P  N  E  K  R  D  H  M  V  L  L  E  F  V

Vertebrate      accgctgctggaatcacacatggcatggacgaactatacaaatag 717
mitochondria    T  A  A  G  I  T  H  G  M  D  E  L  Y  K  *
```

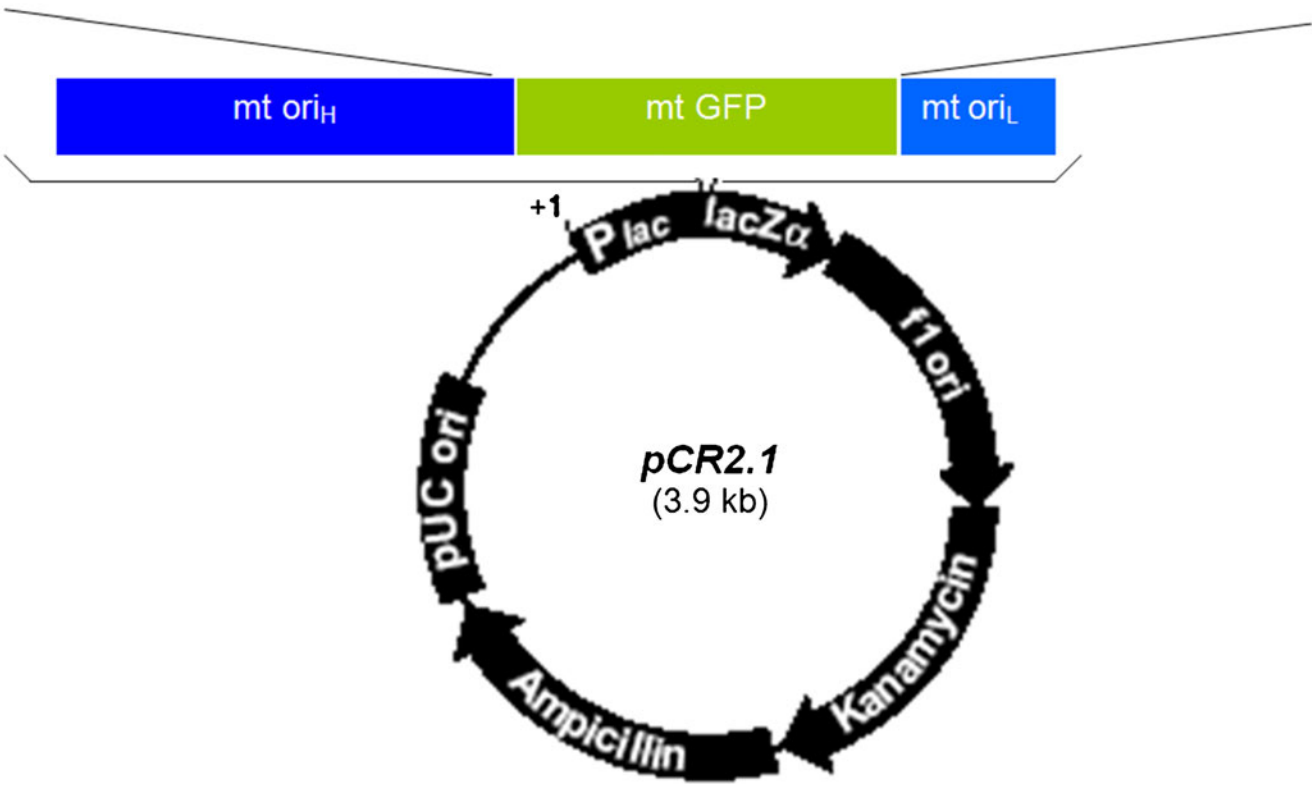

Fig. 1 Strategy used to construct pmtGFP. *A* Alignment of nucleotide sequence of mtgfp and its translation is shown. An early termination was expected at codon 57 (nt169-171) if GFP was translated in the cytosol (universal codon tga is a stop codon) as opposed to a full length version GFP if translated in vertebrate mitochondrion (mitochondrial codon tga is tryptophan, W). *B* The 12 overlapping oligonucleotides used for creating the mtgfp fragment were 46–100 nt in length (Table 1) and their positions are indicated by *arrows*.

Table II PCR Primers Used to Generate the Final pmtGFP Construct

Fragments	Primer code	Sequence 5′→3′[a]
Fragment 1 mtc (mtO_H)	mtcL3584 (30nt)	GACCTCTGGGAGCTCGAAGAAGGAGCTACT
	mtcH1057 (30nt)	***TGGTCATGCGGCCGCATTATAA***GGCCAGGA
	mtcL1036 (30nt)	***TTATAATGCGGCCGCATGACCA***ATGAACAC
Fragment 2 mtc(mtGFP)	mtcH2687 (30nt)	***CATGGTACCGTCGACCCTGGCTCT***GCCACC
	mtcL2464 (30nt)	***AGAGCCAGGGTCGACGGTACCATG***AGCAAA
	mtcH3424 (30nt)	AT***CTAGTTGAGGTCCTCGGTACCCTATTTG***
Fragment 3 mtc (mtO_L)	mtcL3393 (30nt)	TA***CAAATAGGGTACCGAGGACCTCAACTAG***
	mtcH15 (30nt)	TCCTTCTTCGAGCTCCCAGAGGTCTTAAGG

[a] Sequences in bold italic indicates overlapping nucleotides between oligonucleotides

fragment (1,038 bp) corresponds to region L15354-L95 of wild-type (wt) mouse mtDNA (GeneBank J01420), encompassing part of the D-loop, tRNAs—Phe and Pro (20). This fragment was amplified by PCR using RAW 264.7 mtDNA as a template and primers mtcL3584 and mtcH1057. The mtO_L fragment (181 bp)was obtained by PCR amplification of RAW264.7 mtDNA using primers mtcL3393 and mtcH15 and corresponds to region 5081–5262 of the wild-type mouse mtDNA, encompassing the mitochondrial O_L region, and tRNAs—Asn, Cys, and Tyr (20). The thermal cycling conditions, described previously, were used to generate mtO_H and mtO_L fragments.

Overlapping mtO_H, mtcGFP, and mtO_L fragments were extracted from agarose gels and purified using a QIAquick gel extraction kit (Qiagen) to prevent carry-over of unincorporated primers. Progressive joining of the three fragments in the order mtO_H–mtcGFP–mtO_L to create the mitochondrial DNA insert was carried out using the modified mega-primer PCR method detailed by Chrzanowska-Lightowlers *et al.* (14) and indicated primers (Fig. 1). Mega-primer PCR reactions containing 2 pmoles each of the 3 PCR fragments and 50 pmoles of specific primers were subjected to thermocycling involving one cycle at 95°C for 4 min, followed by 35 cycles at 95°C for 1 min, annealing for 1 min and extension at 72°C for 1 min, and then a single cycle at 72°C for 10 min. Following mega-primer PCR, the mtc fragment (1,996 bp) was purified and cloned into the TA vector pCR2.1 (Invitrogen) according to the manufacturer's guidelines.

Ligation products were transformed into competent *E. coli* cells by heat shock (INVαF cells, Original TA Cloning Kit, Invitrogen) and white colony transformants selected for resistance to ampicillin (50 μg/mL). Plasmid DNA was isolated from 250 mL overnight cultures using the maxi (EndoFree Plasmid Maxi Kit, Qiagen, Australia) plasmid purification kit, respectively. Clones with the expected mtO_H–mtcGFP–mtO_L insert in the correct orientation were identified using a combination of PCR, restriction enzyme digestion and DNA sequencing analyses.

Cell Lines Used in Transfection Studies

Unless specifically stated, the cell lines used for transfection studies were grown in six well plates or on coverslips in 35 mm culture dishes and maintained in Dulbecco's modified Eagle's medium (DMEM) supplemented with 10% fetal bovine serum (FBS), 100 IU/mL Penicillin, 100 μg/mL Streptomycin and 1 mM L-glutamine at 37°C in a humidified atmosphere containing 5% CO_2. Cells were grown to 75% confluence and used for transfection assays.

The RAW 264.7 macrophage cell line was a kind gift from Dr. Tedjo Sasmono, IMB-UQ, Brisbane, Australia. Cells seeded in 100 mm culture dishes (Nunc) or on coverslips were grown in RPMI 1640 supplemented with 10% fetal bovine serum, 2 mM L-glutamine, and 100 U/mL of Penicillin-Streptomycin (PenStrep).

The OKO160 (OKO) mouse embryonic stem cell line (21) contains a targeted insertion of a lacZ/neo gene fusion inserted into the Oct3/4 gene. OKO cells were provided by Dr. Martin Pera, Australian Stem Cell Centre (ASCC), Monash University, Australia. The OKO cells were maintained on gelatin-coated dishes without feeder cells in DMEM supplemented with 10% FBS, 0.1 mM 2-mercaptoethanol (Sigma Chemical Co., St. Louis, MO, USA), 0.1 mM non-essential amino acids and 1,000 U/mL of leukemia inhibitory factor (LIF; Chemicon Australia).

Mouse fetal neuronal stem (mFNS) cells were derived from day 12–14 embryos created from matings of F1 (C57bl × CBA) female mice with Zin40 129 Sv 12 B/c males. Fresh primary mFNS cells were plated at a density of 5×10^5 in 2 mL Neurobasal A (NA) media containing 1% of ITS-G (100X); 1% CDL (100x); 1% N2 (100X); 1% B27 (50X); 10 ng/mL EGF; 10 ng/mL bFGF; 200 U/mL Penicillin 200 μg/mL Streptomycin and 0.5 mM L-glutamine.

A primary culture of rat fetal fibroblast cells was provided by from Dr. Shahnaz Fida, Monash Institute of Medical Research (MIMR), Australia. Cells were maintained in a humidified atmosphere of 5% CO_2 at 39°C.

A bovine fibroblast cell line derived from a cloned bovine 'Rameses' was obtained from Dr. Andrew French, Animal Biotech Group, MIMR, Australia. Cells from passage 12 were cultured in a humidified atmosphere of 5% CO_2 at 39°C.

The human kidney 293 cell line was provided by Dr. Martin Pera, ASCC, Australia.

Transfection Assays

GFP expression plasmid vectors pHygEGFP (a gift from Dr. Martin Pera), pNVFEGFP (a gift from Dr. Tedjo Sasmono) and the pmtGFP construct were used in transfection assays of mammalian cell lines.

Standard transfection assays were performed on RAW264.7 cells using the Lipofectin transfection system (Invitrogen) as indicated by the manufacturer. Lipofectin-DNA complexes were formed by mixing 7.5 μL of Lipofectin with 1 μL (100 ng) of plasmid DNA. DQAsomes for mitochondrial transfection were prepared as described by Weissig *et al.* (7). Briefly, dequalinium chloride (Sigma, Australia) (10 mM final concentration) was dissolved in a sterile tube in methanol and the organic solvent removed under a stream of nitrogen. The resulting thin films were resuspended in deionized water, vortexed and sonicated in a Branson bath sonicator for 30 min until a clear opaque solution was obtained. The solution was then centrifuged at 3,000 rpm for 30 min and the resulting supernatant collected. DQAsomes were used within 24 h of preparation. RAW264.7 cells were transfected by adding 45 μL of DQAsome-DNA complex (126 μM DQAsome, 138 ng pmtGFP) directly into 1.5 mL of culture media. Dishes were incubated for 2 h, the transfection media then replaced with 1.5 mL of fresh media and further cultured. Following transfection, media were replenished every second day.

Prior to transfection, OKO mouse embryonic stem cells, mFNS cells, rat and bovine fibroblasts and human kidney 293 cells were equilibrated in 1.5 mL of fresh culture media for 2 h. A 10 μL aliquot of DQAsome-DNA complex (13 μM DQAsome, 14 ng plasmid DNA) was then added to the media and dishes incubated for an hour. Following transfection, media was replaced by 1.5 mL fresh culture media containing 200 mM pyruvate and 50 μM uridine. For the mFNS cells, the media also contained 1% KOS (Knock Out Serum, Gibco-Invitrogen).

Assessment of DQAsomes Cytotoxicity

To determine the effects of DQAsomes on growth of the RAW 264.7 macrophage cell line, 2.75×10^4 cells were seeded into 35-mm tissue culture dishes and incubated overnight. The medium was then removed and replaced with fresh media 1 h prior to the addition of defined amounts of DQAsomes. After 5 or 12 h exposure to DQAsomes, cells were washed in PBS and then cultured further in fresh media. Cell growth was observed daily by counting cells in the same grid area. A total of five different areas were counted to determine changes in the cell population for each dish. Cell viability tests on these cultures were also performed using Trypan Blue exclusion.

Epifluorescence Microscopy

Following transfection, cultured cells were periodically visualized for green fluorescence using a Leica DMR epifluorescence microscope equipped with a 100× objective and a GFP fluorescence filter set (470 excitation and 525 nm emission). Digital images were acquired using a digital low light level fluorescence imaging Leica DC200 or DC viewer and processed using Adobe Photoshop version 6 (Adobe Systems Inc., Mountain View, CA).

Flow Cytometry Analysis

The efficiency of transfection observed as the proportion of fluorescent and non-fluorescent RAW264.7 cells was analyzed on day 10 post-transfection using flow cytometry. Cultured cells treated with either DQAsomes or DQAsome-pmtGFP complexes were washed in PBS and detached from the culture dish. Following centrifugation at 3,000 rpm, cells were resuspended in 2% FCS/PBS and immediately analyzed by flow cytometry (Mo-Flo, Cytomation, Ft Collins, CO, USA or FACS Calibur, Becton Dickinson Immunocytometry Systems) equipped with a focused argon laser (488 nm excitation and 525 nm emission). The cut-off defined for GFP positive cells (green fluorescence) and GFP negative cells (no green fluorescence) was determined from FACS profiles obtained from cells treated with DQAsomes only.

Confocal Microscopy

Transfected cells on cover slips were fixed using 4% paraformaldehyde/PBS and the cover slip placed on a glass slide. Observations were made on a Bio-Rad MRC1000 confocal microscope, Ar Kr/Ar 488 with a 200× objective and T1 triple dichroic, T2A 560 DRLP/500 DCLP filter set. Digital images were acquired with an FITC filter set (488 nm excitation and 522–535 nm emission). In depth pictures were taken 4 times in a Z-series using a Kalman filter and scanning, then analyzed with Confocal Assistant version 4.02.

Immunohistochemistry

RAW264.7 cells transfected with DQAsome-pmtGFP complexes (d3-d12 post-transfection) were immunostained with

an anti-GFP monoclonal antibody (mouse anti-GFP mAb, Sigma) using standard immunoperoxidase methods and diaminobenzidin for color development (22). Stained cells on coverslips were mounted using Vectashield (Vector), and examined microscopically for brown stained particles (Axiophot microscope; Zeiss, Germany).

To confirm that the green fluorescence observed in DQAsome-pmtGFP transfected RAW264.7 cell originated from GFP expression, simultaneous experiments of epifluorescence microscopic observation and GFP immunostaining were performed on DQAsome-pmtGFP transfected cells. Transfected cells (d3-d12 post-transfection) were fixed in 4% formaldehyde for 20 min and after washing with PBS for 10 min mounted on slides using Vectashield. Treated slides were then examined for green fluorescence under an epifluorescence microscope (Axiophot, Zeiss Germany). Images of cells exhibiting green fluorescence were captured using the Zeiss microscope camera and positions marked by coordinates. The same slides were subsequently immunostained with the anti-GFP mAb as described previously. Stained cells were examined microscopically and images were captured using the microscope camera. Using coordinates, images of epifluorescence and GFP staining were compared for concordance.

Double immunostaining for GFP and the mitochondrial protein NDUFS1 (23) was performed to assess the cellular localization of GFP protein in RAW264.7 cells transfected with DQAsome-pmtGFP complexes. First, GFP immunostaining was performed using the immunoperoxidase method as described above. After microscopic analysis of the slides for brown stained cells, coverslips were retrieved for NDUFS1 staining. A primary rabbit anti-NDUFS1 polyclonal antibody (kindly provided by S. Malik, Eijkman Institute, Jakarta, Indonesia) was employed in a standard alkaline-phosphatase immunostaining protocol (22). Color was developed using 0.4 mg/mL naphtol AS-MX phosphate (Sigma) containing levamisole (Sigma) plus nitro-blue tetrazolium (NBT, 0.6 mg/mL, Sigma) in 0.1M Tris–HCl (Sigma) pH 8.2 to produce a blue precipitate. Stained cells were examined microscopically and images recorded.

Isolation of Mitochondria

Mitochondria from transfected RAW264.7 cells were isolated as described by Towers *et al.* (24) except that the cells were disrupted using three cycles of liquid nitrogen freeze-thaw. The final mitochondrial pellet was resuspended in mitochondrial isolation buffer (24).Isolated mitochondria from $\sim 3 \times 10^5$ cells were resuspended in 15 μL of 1X DNAse I buffer containing 75 U DNAse I. DNAse I treatment was allowed to proceed for 1 h at 37°C to remove any extraneous DNA bound to the outside of the mitochondria. The mitochondrial suspension was subsequently centrifuged at 10,500 rpm for 10 min. The pellet was resuspended in 15 μL of Tris-Cl buffer and a 5 μL aliquot of supernatant kept in a fresh PCR tube to monitor the efficiency of DNAse I digestion. The 10 μL of remaining suspension and the 5 μL aliquot were both heated at 75°C for 5 min to inactivate DNAse I. Mitochondrial lysis was completed by 3× freeze-thaw cycles in liquid nitrogen. Following centrifugation at 10,500 rpm for 10 min, the supernatant was used as a template for PCR assays of pmtGFP and mtDNA sequences.

PCR and RT-PCR Analysis of Transfected Cells

PCR was used to detect the presence of pmtGFP sequences and wt mtDNA sequences *cox2*, *atp6* and *cytb* in whole cell lysates or in mitochondria isolated from DQAsome-pmtGFP RAW264.7 transfected cells. PCR reactions were as described previously and performed using cycle conditions of 94°C for 5 min, followed by 30 cycles of denaturation at 94°C for 30 s, annealing at 50–60°C for 30 s, extension at 72°C for 30 s, then a final extension at 72°C for 10 min, on the Gene amp 7100 PCR machine. Primer pairs for the amplification of *cox2*, *atp6* and *cytb* wt mtDNA sequences are shown in Table III.

Reverse transcription (RT) reactions on whole cell lysates was also performed to detect mtgfp specific mRNA. Transfected cells were detached from the culture dish and collected in 100 μL PBS. A 10 μL volume of cell suspension (~4,000 cells) was used for RT-PCR using Cells to cDNA Kit (Ambion) according to the manufacturer instructions. Total RNA was converted to cDNA by a random decamer primed RT reaction. Internal *mtgfp* sequence primers (mtGF266s and mtGR421s) or wt mtDNA primers (Table III) were in specific PCR reactions. Products were resolved on 2% ethidium-bromide agarose gels and images captured under UV light.

Fluorescence *In Situ* Hybridization (FISH)

To assess the localization of pmtGFP DNA, FISH assays were performed at 48 h or 1–2 weeks post-transfection. Transfected cells were fixed on slides, hybridized with fluorescently labeled pmtGFP and/or wt mtDNA probes and then counterstained with nuclear stain Hoechst 33342. The 155 bp *mtgfp probe (*prepared with mtGF266s and mtGR421s primers) and the 167 bp*cox2* probe (prepared with the L7206 and H7373 primer pairs) were generated by PCR (Table III) and purified using Qiagen PCR purification columns (Qiagen). The *mtgfp* and *cox2* probes were labeled by nick translation with Alexa Fluor 532 and Alexa Fluor 568, respectively (Nick Translation System, Promega, and ARES DNA Labelling kit, Molecular Probes, Inc). FISH assays were performed as described by Margineantu

Table III General PCR Primers for Molecular Analyses

Fragments	Primer code	Sequence 5′→3′	Amplicon (bp)
mtgfp short/internal primers (20 nt)			
	mtGF1s	GAGGGTACCATGAGCAAAGG	160
	mtGR160s	GGAGTTTTCCGGTGGTGCAG	
	mtGF140s	CTGCACCACCGGAAAACTCC	148
	mtGR287s	CGTTCTTGTACGTAGCCTTC	
	mtGF266s	CCGAAGGCTACGTACAAGAA	155
	mtGR421s	GTTTGTGGCCGAGGATGTTT	
	mtGF401s	GAAACATCCTCGGCCACAAA	142
	mtGR542s	TGGTCGGCTAGTTGTACGGA	
	mtGF522s	ATCCGTACAACTAGCCGACC	155
	mtGR677s	GCGGTTACAAATTCAAGTAG	
	mtGF654s	GTCCTACTTGAATTTGTAAC	72
	mtGR726s	CTCGGTACCCTATTTGTATA	
wtmtDNA primers			
cox2	L7206	GAACTATTCTACCAGCTG	168
	H7373	ATGAATCAAAGCATAGG	
atp6	L8031	ACGCCTAATCAACAACC	224
	H8254	CTCATAGTGGAATGGC	
cyt b	L14363	CGGGTGACTAATCCG	156
	H14518	GCTGTGGCTATGACTGC	

et al. (25). Fluorescent signals were visualized using the epifluorescence microscope with GFP and Texas Red fluorescence filter sets.

RESULTS

Generation of the Minimitochondrial Plasmid pmtGFP

The strategy used to construct the mini-mitochondrial plasmid pmtGFP is outlined in Fig. 1. The *gfp* sequence was first recoded to adjust to the mitochondrial codon system and to ensure exclusive intramitochondrial synthesis of green fluorescence protein. The favoured mitochondrial codons that are highly expressed in mitochondrial-encoded proteins were used to replace the corresponding codons of an optimized human expression *gfp* gene (EGFP) (GI:1289497, accession U50963) to facilitate mitochondrial expression of GFP (19). Twelve contiguous primers incorporating all the required nucleotide alterations (Table I) were used to generate a mitochondrial coding *mtgfp* gene, each having overlapping sequences at 5′ and 3′ end. Using these overlapping primers, multiplex PCR was performed to engineer *mtgfp*. The final fragment (717 bp) was cloned independently into the vector pCR2.1, facilitating the production of the full-length mtcGFP sequence as detailed in Fig. 1. DNA sequencing verified the correct mitochondrial codons in the artificial *mtgfp* fragment. Using the megaprimer PCR technique, the *mtgfp* fragment was joined with the other fragments, mtO_H and mtO_L, to form the mtc construct which was subsequently inserted into the plasmid pCR2.1 by TA cloning. A total of 10 white clones out of 70 were found to be positive for the insert. Following confirmation using PCR and restriction enzyme analysis the correct sequence of the mtO_H–mtcGFP–mtO_L insert was reconfirmed by DNA sequencing and one clone designated pmtGFP was chosen as the final construct.

Transfection of RAW264.7 Cells with pmtGFP

To assess the degree of nuclear-cytoplasmic GFP expression, transfection assays were performed using Lipofectin lipoplexes to deliver pmtGFP or the control plasmid pHygEGFP into the nuclei of RAW 264.7 cells. The plasmid pmtGFP, constructed for mitochondrial expression of GFP, has a substitution of TGG (tryptophan) to TGA at codon 57 in the GFP sequence which was specifically designed to terminate any possible nuclear expression of GFP. Analysis of pmtGFP transfected cells by FISH (155 bp GFP probe derived from the mtGF266s-mtGR421s region of the mtgfp fragment) and Hoechst staining showed that plasmid DNA was localized to the nuclear region with nuclear delivery efficiency of approximately 89%. Following transfection, epifluorescence microscopy failed to detect any green fluorescence in the nucleus or cytosol above a low background seen in non-transfected cells (Fig. 2). As expected, strong green fluorescence was detected in the nucleus and throughout the cytoplasm of cells transfected with the positive control plasmid pHygEGFP. These experiments demonstrate that delivery of pmtGFP to the

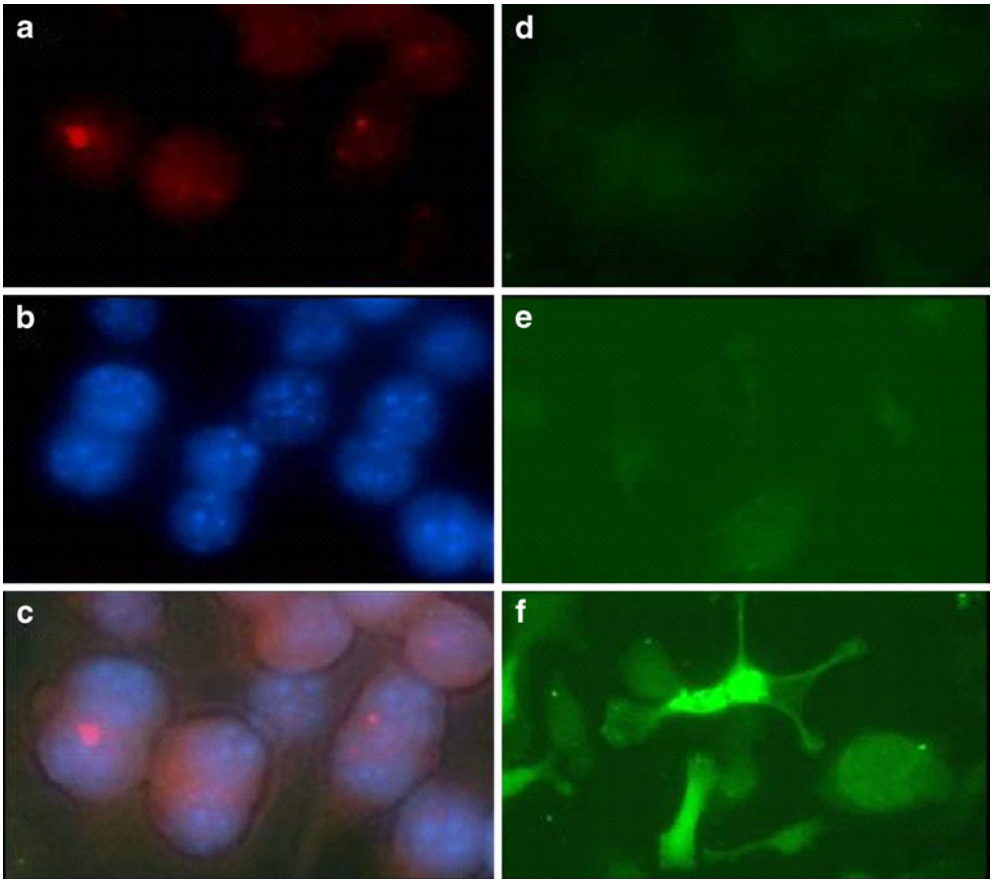

Fig. 2 Localization of pmtGFP and its expression following transfection into RAW 264.7 cells. To assess pmtGFP localization and *mtgfp* expression following Lipofectin transfection, FISH assays and epifluorescence microscopy observations were performed on transfected cells. Transfected cells were fixed on slides and hybridized to an ALEXA red fluorescently labeled pmtGFP probe (**a**) and counterstained with Hoechst 33342 for nuclear staining (**b**). The pmtGFP plasmid was delivered into the nuclei of the cells as seen in the merged image (**c**). The nuclear delivery of pmtGFP did not result in any green fluorescence above b ackground (**d**). Cells transfected with pHygEGFP, carrying a nuclear encoded *gfp* gene, served as the positive control for green fluorescence (**f**) Non transfected cells served as a negative control (**e**).

nucleus does not culminate in nuclear or cytoplasmic expression of GFP.

In preliminary mitochondrial transfection studies, RAW 264.7 cells were exposed for 2–12 h to various DQAsome concentrations, with and without different amounts of pmtGFP DNA, to determine the optimal conditions for mitochondrial DNA transfection. A high degree of cytotoxicity was apparent in the cell cultures for several days following DQAsome treatment and removal. In general, the rate of cell growth was reduced as the concentration of and exposure to DQAsome increased. Initially, the amount of dead cells increased steadily for 3–4 days, but after further culture, some cells recovered from the cytotoxicity and survived. These cells continued to grow and formed colonies. The recovery time depended on the concentration and time of exposure to DQAsome. For the purpose of mitochondrial transfection in RAW 264.7 cells, DQAsome exposure at a concentration of 126 μM for 2–3 h incubation was used in RAW264.7 experiments. Although these conditions were still toxic to the cells, they were effective for DNA delivery.

Time lapse observations of green fluorescence in transfected RAW 264.7 cells were undertaken using four different regimes; namely (a) no transfection, (b) DQAsome transfection, (c) DQAsome-plasmid vector transfection (pmtGFP without *mtgfp* gene) and (d) DQAsome-pmtGFP transfection. Expression of GFP was examined at days 2, 3, 7, 14, 25 and 30 post-transfection using epifluorescence microscopy. At day 1 after transfection, all cells exhibited green fluorescence whether treated with DQAsome, DQAsome-plasmid vector or DQAsome-pmtGFP (Fig. 3a). One possible explanation for this phenomenon is that the dequalinium used to prepare the DQAsome exhibits intrinsic 'autofluorescence'. Nevertheless, following further culture, background green fluorescence in DQAsome and DQAsome-vector treated cells diminished with time. By day 3, only a small number of DQAsome-pmtGFP transfected cells (<1%) exhibited significant green fluorescence. After 3 days, cells treated with either DQAsome or DQAsome-vector showed minimal autofluorescence, whereas cells treated with DQAsome-pmtGFP demonstrated a markedly more intense green fluorescence. Under the imaging conditions for visualization of green fluorescence, confocal microscopic observations revealed that the green fluorescence appeared as punctate structures scattered within the cytoplasm, whereas the nuclei of cells showed no green fluorescence (Fig. 3b). Together, these findings demonstrate that the prolonged fluorescence observed in DQAsome-pmtGFP transfected cells did not result from DQAsome or DQAsome-vector complexes and supports

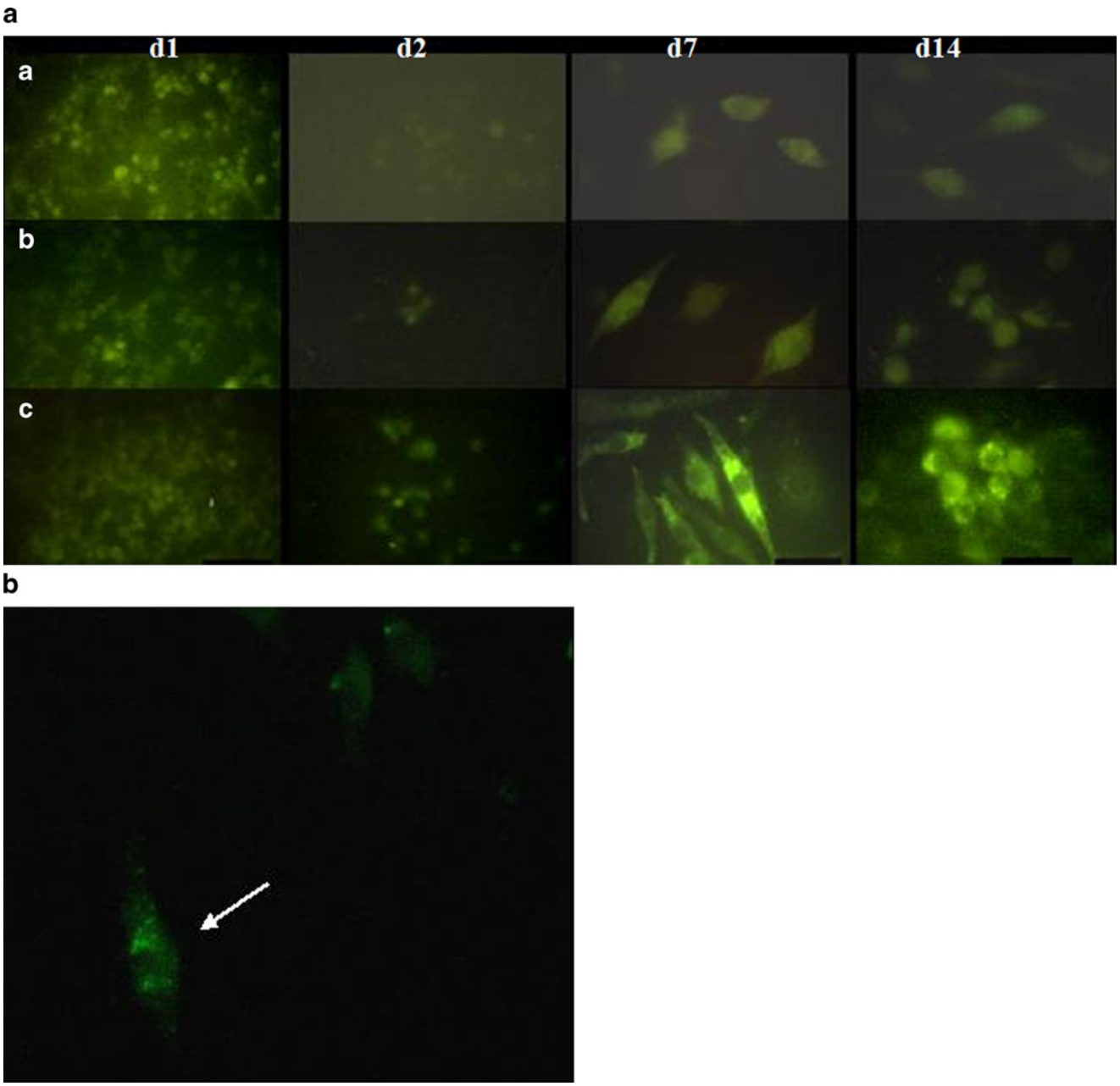

Fig. 3 (**a**)Time course observations of the green fluorescence in transfected cells. Epifluorescence observations on RAW 264.7 cells were made at different days (d) post-transfection with DQAsome alone (*a*), DQAsome-plasmid vector (*c*) and DQAsome-pmtGFP (*c*). Green fluorescence was detected initially in almost all cells (d1) which then diminished with time except in pmtGFPtransfected cells. Images are shown at different magnification (d1, 200×; d2, ×400; d7 and d14, 1000×) to better illustrate the intensity of the green fluorescence and its cellular distribution. (**b**) Confocal microscopic observations of DQAsome-pmtGFP transfected cells. Shown here is a flattened image of 8 of 21 optical z sections of transfected RAW264.7 cells, with 1 μm increments. The green fluorescence appeared as dot-like structures, randomly in the cytoplasm of the cell (*arrow*). The nuclear region did not showing any green fluorescence. Confocal microscopy images were taken at 200× magnification and 4× zoom.

the notion that the observed green fluorescence results from the transfected pmtGFP construct.

Validation of Mitochondrial-Based GFP Expression

The punctate pattern of green fluorescence observed in the cytosol of pmtGFP transfected cells suggested that GFP expression was mitochondrial based. To confirm this, co-localization experiments were performed using a red-labelled pmtGFP FISH probe. In the first experiment, cultures containing green fluorescent cells (1–2 weeks post-transfection) were fixed and hybridized with the pmtGFP red probe. Co-localization of green fluorescence with red FISH fluorescence was observed in the cytoplasmic region

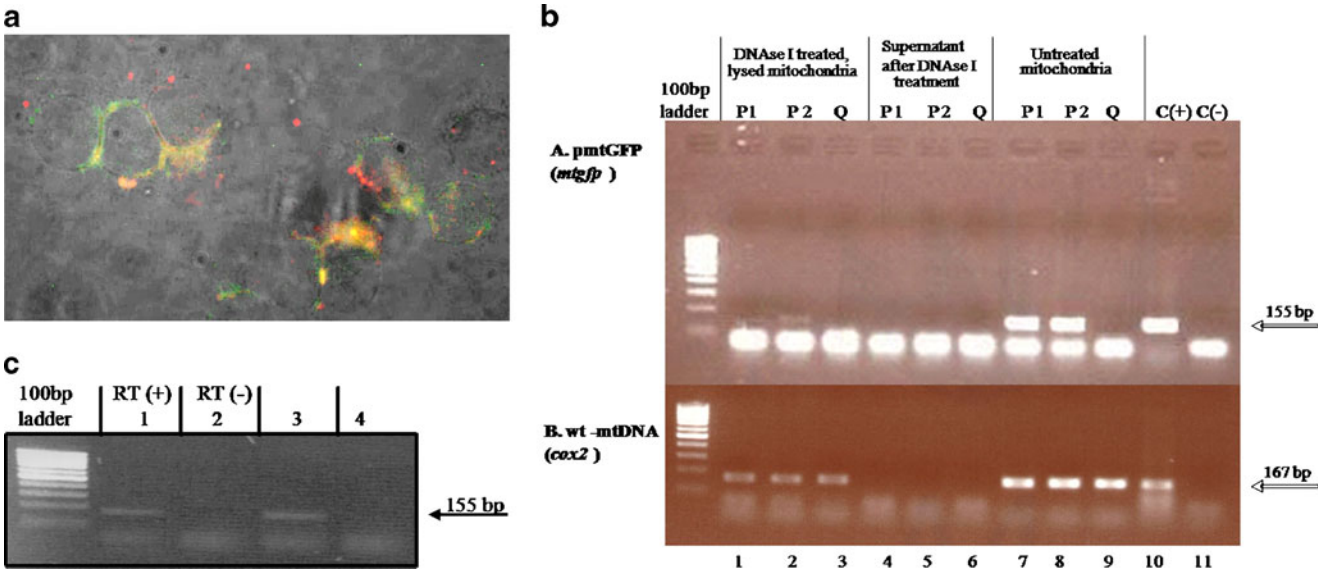

Fig. 4 (**a**) Colocalization of pmtGFP with wt mtDNA in transfected cells. The distribution of plasmid pmtGFP FISH signal (red fluorescence) was compared to that produced by the wt mtDNA FISH signal (green fluorescence). Colocalization of the two DNA signals (yellow fluorescence) was observed in 1–5% of the transfected cells. (**b**) *PCR detection of pmtGFP in purified mitochondria.* PCR assays were performed on mitochondria isolated from DQAsome-pmtGFP transfected (G1: 63 μM DQAsome-69 ng pmtGFP; G2: 126 μM DQAsome-138 ng pmtGFP) and DQAsome treated (Q) cells. The mtGF266s-GR421s and L7206-H7373 primer pairs (Table III) were used to amplify a 155 bp internal fragment of *mtGFP* (*A*) and a 167 bp fragment of *cox2* (wt-mtDNA) (*B*), respectively. Lanes 1–3 DNase I treated, lysed mitochondria: isolated mitochondria were treated with DNAse I, heated at 95°C for 5 min to inactivate DNAse I and to lyse mitochondria, lanes 4–6: supernatant of lanes 1–3 after DNAse I treatment, lanes 7–9: isolated mitochondria not treated with DNAse I, lane 10: pmtGFP DNA positive control and lane 11: water negative control. Expected bands are indicated by *arrows*. The demonstration of a pmtGFP signal in DNase I digested fraction of mitochondria (*A*, lane 2) indicates that some exogenous pmtGFP was internalized into the mitochondria following transfection with pmtGFP. (**c**) RT-PCR analysis of mtgfp expression. RT-PCR assays were performed to determine whether *mtgfp* was expressed by the transfected cells. Primer pair mtGF266s and mtGR421s (Table III) was used to detect an internal *mtgfp* fragment of 155 bp. Lanes 1–2 PCR products from transfected RAW264.7 cells with and without RT; lane 3 pmtGFP DNA positive control and lane 4 water negative control.

(data not shown). In a double staining FISH assay using a green-labelled wt mtDNA probe and the red-labelled pmtGFP probe, co-localization of signals observed as yellow fluorescence was also observed as discrete spots in the cytoplasm (see Fig. 4a for typical staining pattern). This co-localization pattern suggested that pmtGFP was delivered to a small fraction of the cellular mitochondria.

To support the FISH assays, PCR was performed in order to demonstrate pmtGFP DNA in mitochondria. Mitochondria were isolated from cultures containing green fluorescent cells and treated with DNAse I to remove any residual pmtGFP plasmid that might still be bound to the outer mitochondrial membrane. PCR analysis of the lysates with gfp primers (mtGF266s-mtGR421s) revealed the expected gfp specific product of 155 bp, indicating that DQAsome can deliver pmtGFP into a DNAse I insensitive location within the mitochondria (Fig. 4b). To further validate the green fluorescence observed in pmtGFP transfected cells, RT-PCR and immunohistochemistry assays were undertaken to confirm that gfp mRNA and GFP protein were indeed expressed. For mRNA analysis, whole cell lysates were treated with DNAse I to eliminate contaminating pmtGFP that could serve as a PCR template in RT-PCR. Following RT-PCR (using mtGF266s and mtGR421s primers) a 155 bp PCR product of the expected size was present in RT positive but not RT negative reactions (Fig. 4c) indicating that the pmtGFP plasmid was transcribed.

Fig. 5 (**a**) Immunostaining for GFP. RAW 264 seven cells transfected with ▶ DQAsome-pmtGFP were stained with anti-GFP antibodies at different times post-transfection (*c*, d3; *d*, d5; e, d7). Granule-like brown particles were indicative of positive staining. Cells transfected with DQAsome and stained with anti-GFP antibodies (*b*) or excluding primary antibody (*a*) served as negative controls. The positive control was pNVFEGFP transfected cells stained with anti-GFP antibodies (*f*). (**b**) Concordance of green fluorescence and anti-GFP immunoreactivity in pmtGFP transfected cells. Green fluorescence signals (*a*) and corresponding GFP-DAB immunoperoxidase reaction (*b*). Images were taken at 1250× magnification. (**c**) Double immunostaining for GFP and NDUFS1 pmtGFP transfected cells. Transfected RAW 264.7 cells were first stained for GFP using the DAB-immunoperoxidase technique (*a*) then for NDUFS1 using NBT-alkaline phosphatase (*b*). Note that the pattern of brown stained GFP in a dividing transfected cell (*arrow*) matches with the punctate dark blue/purple of staining for NDUFS1 (*A* and *B*, respectively). Control experiments were cells treated with DQAsome-only similarly stained for GFP and NDUFS1(*c*), normal (non-treated) cells stained for NDUFS1 (*d*). An antibody negative control is shown in panel *E*. Images were taken at 1250× magnification.

To detect GFP protein and demonstrate mitochondrial localization of pmtGFP, a series of immunohistochemical assays were performed using an anti-GFP monoclonal antibody. Immunohistochemistry for GFP performed at different times after transfection demonstrated a speckled pattern of brown immunoprecipitates in the cytoplasmic region (Fig. 5a). Specific staining was evident as early as day 3 after transfection and increased in intensity with time.

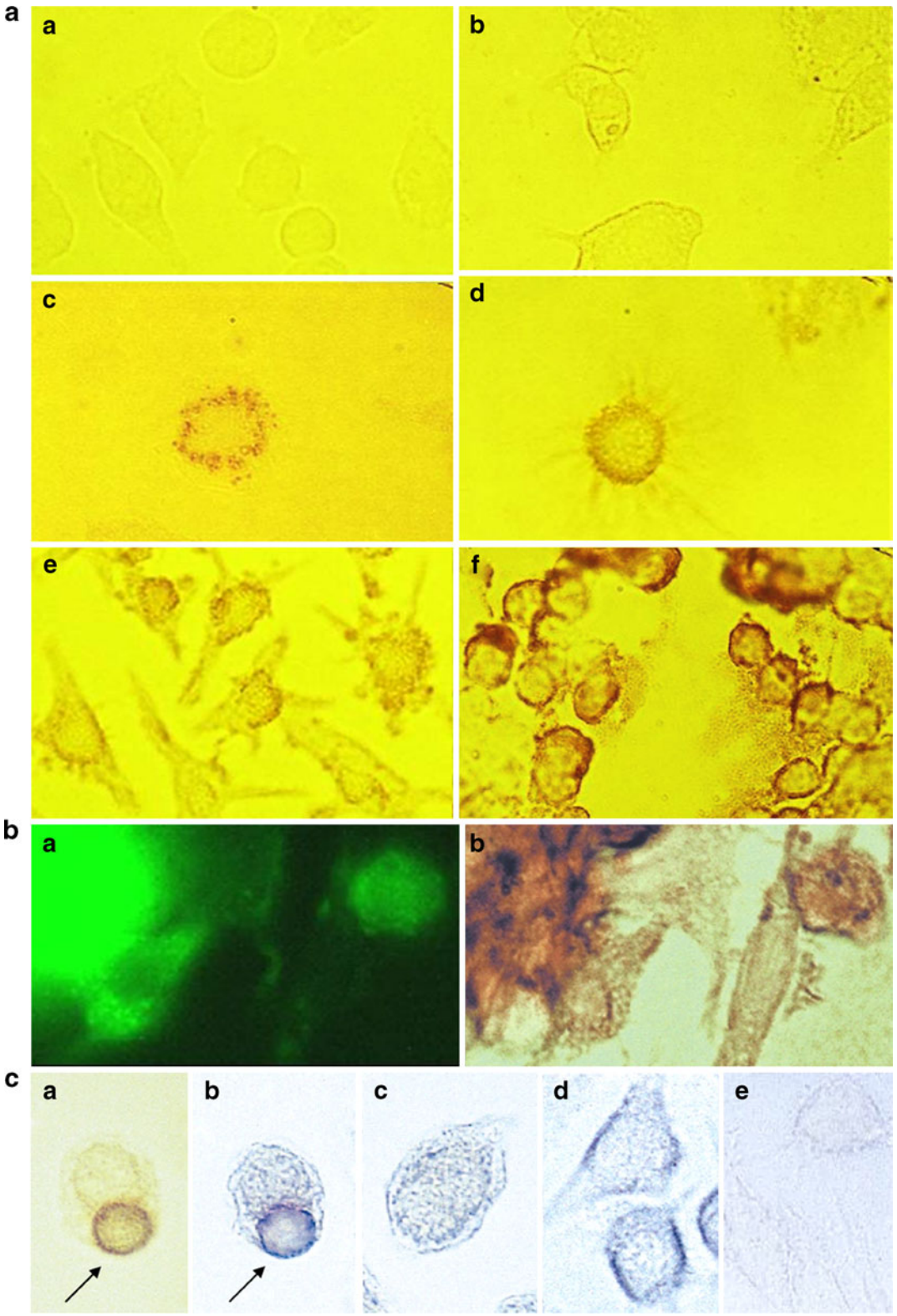

These observations correlate well with epifluorescence studies of the temporal expression of the green fluorescence in RAW264.7 cells post-transfection (see Fig. 3). More definitive experiments in which the expressed GFP was detected in the same cells by both epifluorescence and immunohistochemistry revealed that the green fluorescence signals coincided with the brown precipitate of GFP protein (Fig. 5b). At higher magnification, granule-like staining was clearly observed in DQAsome-pmtGFP transfected cells. In contrast, and as expected, control cells transfected with Lipofectin-pNVFEGFP exhibited uniform staining throughout the entire cytoplasm of the cells (Fig. 5a). The mitochondrial location of the GFP was finally confirmed by double immunostaining experiments using anti-GFP antibodies and antibodies to a well studied mitochondrial protein NDUFS1 (a subunit of the respiratory complex I), (23). As shown in Fig. 5c the brown staining for the GFP observed in transfected cells co-localized with the blue signal of NDUFS1. Hence the collective observations of immunohistochemistry from these experiments strongly indicate that the GFP expression in DQAsome-pmtGFP transfected cells is associated with the mitochondria.

Efficiency and Stability of Mitochondrial GFP Expression

An accurate assessment of transfection efficiency was determined by using fluorescent activated cell sorting on days 1, 3, 10 and 14 after transfection. In five experimental replicates, only a small percentage of cultured cells (range of 0.16 to 11.4%, Fig. 6) showed green fluorescence after 14 days transfection. In all cases, the percentage of GFP positive cells increased over time following transfection.

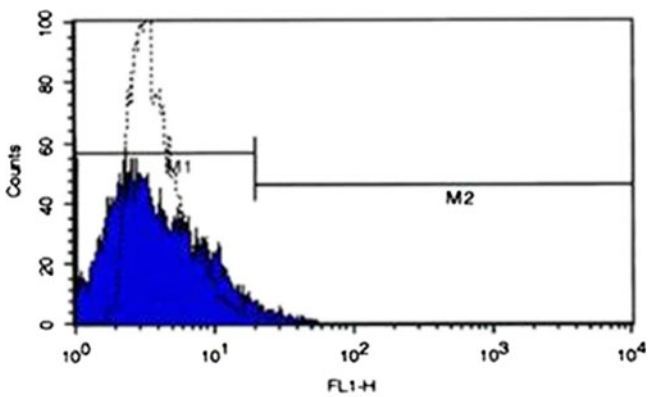

Marker	Left, Right	Events	% Gated
All	1, 9910	7959	100.00
M1	1, 20	7806	98.08
M2	20, 9910	157	1.97

Fig. 6 FACS analysis of RAW 264.7 cells transfected with pmtGFP. Transfected cells (blue curve), representing 1.97% of total cells showed significant green fluorescence (M2 region) compared to DQAsome-only treated RAW 264.7 cells (transparent curve, dotted line). FACS was performed on cells cultured for 10 days following transfection.

To determine whether the transfected RAW264.7 cells maintained the introduced pmtGFP construct after continuous culture, PCR analysis was performed on mitochondria isolated from transfected RAW 264.7 cells. Isolated mitochondria cells were treated with DNAse I, lysed and then subjected to PCR using gfp—and mtDNA specific primers. The pmtGFP and wt mtDNA sequences could be detected in the mitochondria of transfected cells following 30 days culture (four subpassages) indicating that the artificial construct could be maintained within mitochondria (Fig. 7).

Mitochondrial Transfection of Different Mammalian Cell Types

The mitochondrial transfection method used to modify mitochondria of RAW264.7 cells was extended to other mammalian cell lines to assess the versatility of the DQAsome transfection method and the functionality of the pmtGFP construct. Epifluorescence microscopy performed on day 3 after transfection showed significant green fluorescence over background in the cytoplasm of transfected OKO mouse embryonic stem cells, mouse fetal neuronal stem cells, rat primary fibroblasts, bovine fibroblasts and human kidney 293 cells (Fig. 8). The degree of DQAsome cytotoxicity post-transfection was markedly different to that seen in RAW264.7 cells which was in the order of an 80% loss of cells. At day 3 post-transfection, there was 60% loss of viability in the OKO ES and mFNS cell cultures, whereas in the fibroblast and kidney cell lines there was only a 20% loss of viability. Nevertheless, the transfection efficiency, as judged by microscopic observation and FACS analysis of the remaining viable cells (data not shown), was variable, ranging from as low as 1% to as high as 5%.

DISCUSSION

In this report we describe the development of a novel strategy for expression of reporter genes in mammalian mitochondria using a DQAsome transfection system and an artificially created mitochondrial genome pmtGFP. The results reported here indicate that the DQAsome transfection system was capable of introducing the pmtGFP into the mitochondria of mammalian cells, albeit at a low level, leading to expression of GFP. The conclusion is based on several inter-related observations. Firstly, FISH assays demonstrated colocalization of the plasmid pmtGFP signals with that of the wt-mtDNA. Secondly, PCR assays showed that the plasmid pmtGFP was detected in mitochondria isolated from transfected cells. Thirdly, RT-PCR assays

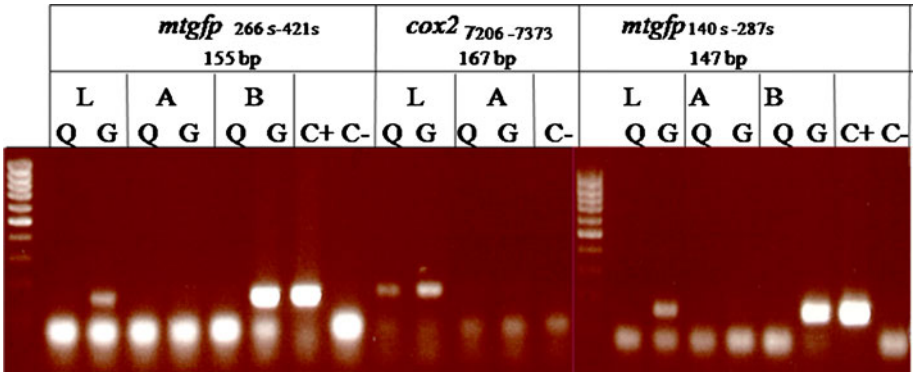

Fig. 7 PCR analysis to determine the preservation of pmtGFP DNA within mitochondria. PCR analysis was performed on mitochondria isolated from transfected cells following 30 days of continuous culture. The isolated mitochondria were used as a template either directly (*B*), or following DNAse I digestion only (*A*) or DNAse I digestion then lysis (*L*) prior to PCR amplification for *mtgfp* and wt mtDNA sequences. The pmtGFP (*mtgfp*) and wt mtDNA (*cox2*) sequences were detected in the mitochondria of DQAsome-pmtGFP transfected RAW264.7 (*G*) indicating that both the artificial and the native mtDNA were maintained within the transfected cells. In the control cells treated with DQAsome (*Q*), only native wt mtDNA was detected.

demonstrated the presence of mitochondrial *mtgfp* transcripts. Fourthly, epifluorescence and confocal microscopic observations revealed the expression of green fluorescence in transfected cells. Fifthly, immunohistochemistry analysis using an anti-GFP monoclonal antibody confirmed that the observed green fluorescence must have originated from newly synthesized GFP protein. Finally, double immunostaining for GFP and NDUFS1, a native mitochondrial protein, demonstrated colocalization of both proteins. Taken together, the combination of molecular and immunoassays provide compelling evidence for the expression of *de novo* GFP mRNA and protein in the mitochondrial compartment following DQAsome transfection of the pmtGFP plasmid.

Given the low efficiency of DQAsome mediated transfection, further improvements to our current protocol are essential. Several modifications are currently being explored to increase the efficiency of mitochondrial transfection. The method used to prepare DQAsome in this study involved sonication of a dequalinium solution to produce a homogeneous liposome reagent. Invariably, it was difficult to reproducibly obtain a homogeneous liposome solution for consistency across all experiments and the prepared DQAsome liposome solution was only stable for up to 96 h. The use of a probe sonicator and the extrusion of particles through a polycarbonate filter of defined pore size (26,27) should facilitate the preparation of a more homogeneous liposome solution and reduce batch to batch variation. Other more stable molecular variants of dequalinium have now been described (28) which would increase the longevity of DQAsome preparations and provide an extra level of quality control. Reduction of DQAsome toxicity is also key issue that needs to be addressed. Two previous studies (29,30) have reported that suramin, a purinergic P(2) receptor antagonist and an anticancer drug, completely prevents apoptosis and necrosis events by antagonizing the effects that dequalinium exerts through a signaling pathway of free radical production and mitochondrial dysfunction (29,30). Hence, addition of suramin prior to and during DQAsome transfection may help to reduce cell toxicity and lead to a significant increase in mitochondrial transfection efficiency.

At present, the DNA delivery mechanism of the DQAsome has not been identified. Similar to the conven-

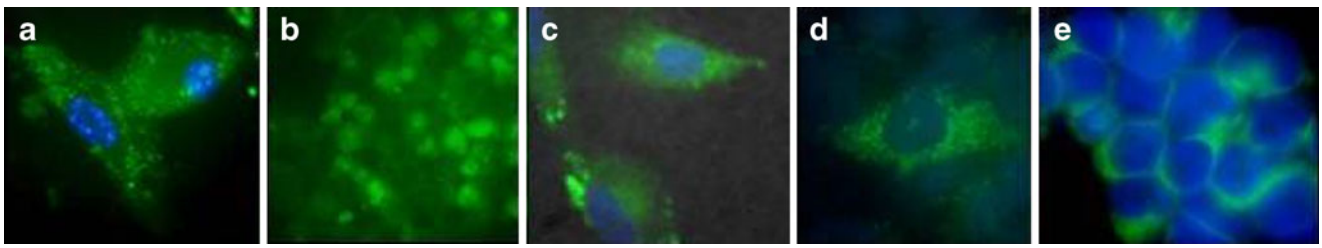

Fig. 8 DQAsome-pmtGFP transfections of different mammalian cell types. Microscopic observations for green fluorescence and blue fluorescence from Hoechst 33342 nuclear staining were completed at day 4 post treatment for mouse fetal neuronal stem cell (**a**), rat fetal fibroblasts (**c**), bovine fibroblasts (**d**) and human kidney 293 cells (**e**), and for OKO ES cells (**b**) were performed following eight passages of single clones. Microscopic observations were evaluated and compared between cells treated with DQAsome-only (not shown) and DQAsome-pmtGFP. The original pictures were taken at 100× magnification, processed and merged using Adobe Photoshop ver.6.0 software.

tional liposome, DQAsome may condense or encapsulate the DNA, carry it across the cell membrane and cytoplasm and then release it into mitochondria. Other cellular mechanisms, analogous to those described for exogenous rRNA (31,32), tRNA (33,34), or DNA (35) may well be at work and facilitate further the internalization of the liposome/DNA complexes into the mitochondria. Investigations to elucidate the mechanism of such DNA internalization would be helpful for the development of better methods for the introduction of exogenous DNA into mitochondria of intact cells.

The ability of DQAsome to mediate the introduction of a minimitochondrial genome into mitochondria could also be applied for the transfer of naturally occurring mitochondrial genomes, rearranged genomes (containing deletions, insertions, or point mutations) or other artificially designed genomes into mitochondria of living cells. Such possibilities would be invaluable to produce cybrid cells and animal models as well as for gene therapy to correct mitochondrial dysfunction caused by mitochondrial genome defects. It is not known, however, whether there is a critical threshold in size and physical structure of the exogenous DNA which would limit the application of this DQAsome delivery system.

The pmtGFP plasmid described here represents the first artificial mitochondrial genome which has been shown to be functional following its introduction into mitochondria of mammalian cells. We hypothesize that mitochondrial expression of the *mtgfp* gene results from mitochondrial complementation between the mini-mitochondrial genome and the wt genome. However, complementation may not be the only mechanism operating to facilitate mitochondrial expression of the *mtgfp*. Another possibility which has not been ruled out in the present study is that mtDNA recombination between the pmtGFP construct and the wt-genome. The identified hotspot rearrangement regions in the mitochondrial genome are near the end of the D-loop, between the replication origins (36). If recombination occurred in these regions then it would transform the pmtGFP construct into a mere insert of the wt-genome. More detailed experiments using Southern blot analysis are required to clarify the existence of such recombination.

Further, studies on the long term expression and maintenance of pmtGFP in mitochondria and the effect on oxidative phosphorylation are essential before such a mitochondrial transfection system can be considered for gene therapy approaches. As seen in patients with mitochondrial diseases involving mtDNA mutations and certain threshold levels of heteroplasmicity to clinically manifest, the number of DNA copies within mitochondria does not always correlates with degree of protein expression. Quantitative studies such as real-time PCR would be necessary to see the dynamics of number and segregation of pmtGFP during mitochondrial replication, mitochondrial fusion-fission and cell division as well as any changes in mtgfp expression. In this study, it was shown that the percentage of GFP positive cells increased over time following transfection. There are several circumstances to explain such observation. First, it is possible that the number of pmtGFP remains the same but segregated to the mitochondria of daughter cells during division. The second possibility is that the protein (mtGFP), concurrently with or without pmtGFP, segregated to the daughter cells. Third, the expression of mtgfp becomes active and increases over time in many cells. Each of these, or combined altogether, may result in the increasing percentage of cells expressing GFP from the exogenous DNA pmtGFP.

CONCLUSION

In conclusion, the generation of a functional artificial mitochondrial genome and the development of the DQAsome transfection method to deliver the construct into mitochondria of intact mammalian cells pave the way for new research on mitochondria. Importantly, the DQAsome and pmtGFP transfection system was successfully applied to a wide range of cells from different mammalian species, confirming the versatility of this newly developed method. Modifications and optimization of the transfection protocol could lead to novel approaches for manipulating the mammalian mitochondria/mt genome. This in turn would facilitate further studies on mitochondria function and dysfunction and the development of innovative strategies for treatment of human mitochondrial diseases.

ACKNOWLEDGMENTS

Dr Diana Lyrawati was supported by a Departmental Scholarship provided by the Monash Immunology and Stem Cell Laboratories, formerly, the Centre for Early Human Development, under the Directorship of Professor Alan Trounson. The authors thank Professor Sangkot Marzuki from the Eijkman Institute for Molecular Biology, Jakarta, Indonesia for providing laboratory resources to perform the immunohistochemistry experiments.

REFERENCES

1. Costanzo MC, Fox TD. Transformation of yeast by agitation with glass beads. Genetics. 1988;120:667–70.
2. Fox TD, Sanford JC, McMullin TW. Plasmids can stably transform yeast mitochondria lacking endogenous mtDNA. Proc Natl Acad Sci USA. 1988;85:7288–92.

3. Johnston SA, Anziano PQ, Shark K, Sanford JC, Butow RA. Mitochondrial transformation in yeast by bombardment with microprojectiles. Science. 1988;240:1538–41.
4. Collombet JM, Wheeler VC, Vogel F, Coutelle C. Introduction of plasmid DNA into isolated mitochondria by electroporation. A novel approach toward gene correction for mitochondrial disorders. J Biol Chem. 1997;272:5342–7.
5. Geromel V, Cao A, Briane D, Vassy J, Rotig A, Rustin P, *et al.* Mitochondria transfection by oligonucleotides containing a signal peptide and vectorized by cationic liposomes. Antisense Nucleic Acid Drug Dev. 2001;11:175–80.
6. Inoki Y, Hakamata Y, Hamamoto T, Kinouchi T, Yamazaki S, Kagawa Y, *et al.* Proteoliposomes colocalized with endogenous mitochondria in mouse fertilized egg. Biochem Biophys Res Commun. 2000;278:183–91.
7. Weissig V, Lasch J, Erdos G, Meyer HW, Rowe TC, Hughes J. DQAsomes: a novel potential drug and gene delivery system made from Dequalinium. Pharm Res. 1998;15:334–7.
8. Weissig V, D'Souza GG, Torchilin VP. DQAsome/DNA complexes release DNA upon contact with isolated mouse liver mitochondria. J Control Release. 2001;75:401–8.
9. Seibel P, Trappe J, Villani G, Klopstock T, Papa S, Reichmann H. Transfection of mitochondria: strategy towards a gene therapy of mitochondrial DNA diseases. Nucleic Acids Res. 1995;23:10–7.
10. Muratovska A, Lightowlers RN, Taylor RW, Turnbull DM, Smith RA, Wilce JA, *et al.* Targeting peptide nucleic acid (PNA) oligomers to mitochondria within cells by conjugation to lipophilic cations: implications for mitochondrial DNA replication, expression and disease. Nucleic Acids Res. 2001;29:1852–63.
11. Flierl A, Jackson C, Cottrell B, Murdock D, Seibel P, Wallace DC. Targeted delivery of DNA to the mitochondrial compartment via import sequence-conjugated peptide nucleic acid. Mol Ther. 2003;7:550–7.
12. Bigger B, Tolmachov O, Collombet J-M, Coutelle C. Introduction of chloramphenicol resistance into the modified mouse mitochondrial genome: cloning of unstable sequences by passage through yeast. Anal Biochem. 2000;277:236–42.
13. Wheeler VC, Prodromou C, Pearl LH, Williamson R, Coutelle C. Synthesis of a modified gene encoding human ornithine transcarbamylase for expression in mammalian mitochondrial and universal translation systems: a novel approach towards correction of a genetic defect. Gene. 1996;169:251–5.
14. Chrzanowska-Lightowlers ZM, Temperley RJ, McGregor A, Bindoff LA, Lightowlers RN. Conversion of a reporter gene for mitochondrial gene expression using iterative mega-prime PCR. Gene. 1999;230:241–7.
15. McGregor A, Temperley R, Chrzanowska-Lightowlers ZM, Lightowlers RN. Absence of expression from RNA internalised into electroporated mammalian mitochondria. Mol Genet Genomics. 2001;265:721–9.
16. D'Souza GG, Rammohan R, Cheng SM, Torchilin VP, Weissig V. DQAsome-mediated delivery of plasmid DNA toward mitochondria in living cells. J Control Release. 2003;92:189–97.
17. D'Souza GG, Weissig V. Approaches to mitochondrial gene therapy. Curr Gene Ther. 2004;4:317–28.
18. Nakamura Y. Codon usage database, GenBank Release 131.0;. http://wwwkazusaorjp/codon/cgi-bin/showcodoncgi?species=Mitochondrion+Mus+musculus+[gbrod], 2002.
19. Zolotukhin S, Potter M, Hauswirth WW, Guy J, Muzyczka N. A "humanized" green fluorescent protein cDNA adapted for high-level expression in mammalian cells. J Virol. 1996;70:4646–54.
20. Bibb MJ, Van Etten RA, Wright CT, Walberg MW, Clayton DA. Sequence and gene organization of mouse mitochondrial DNA. Cell. 1981;26:167–80.
21. Friedrich G, Soriano P. Promoter traps in embryonic stem cells: a genetic screen to identify and mutate developmental genes in mice. Genes Dev. 1991;5:1513–23.
22. Hofman F. Immunohistochemistry. Current protocols in immunology, vol. 1, New York: John Wiley and Sons; 1996. sect. 5.8.1–5.8.23.
23. Malik S, Sudoyo H, Marzuki S. Microphotometric analysis of NADH-tetrazolium reductase deficiency in fibroblasts of patients with Leber hereditary optic neuropathy. J Inherit Metab Dis. 2000;23:730–44.
24. Towers N, Dixon H, Kellerman M, Linnane A. Biogenesis of mitochondria. 22. The sensitivity of rat liver mitochondria to antibiotics; a phylogenetic difference between a mammalian system and yeast. Arch Biochem Biophys. 1972;151:361–9.
25. Margineantu DH, Brown RM, Brown GK, Marcus AH, Capaldi RA. Heterogeneous distribution of pyruvate dehydrogenase in the matrix of mitochondria. Mitochondrion. 2002;1:327–38.
26. Elorza B, Elorza MA, Sainz MC, Chantres JR. Comparison of particle size and encapsulation parameters of three liposomal preparations. J Microencapsul. 1993;10:237–48.
27. MacDonald RC, MacDonald RI, Menco BP, Takeshita K, Subbarao NK, Hu LR. Small-volume extrusion apparatus for preparation of large, unilamellar vesicles. Biochim Biophys Acta. 1991;1061:297–303.
28. Weissig V, Lizano C, Ganellin CR, Torchillin VP. DNA binding cationic bolasomes with delocalized charge center A structure-activity relationship study. STP Pharma Sci. 2001;11:91–6.
29. Chan CF, Lin-Shiau SY. Site of action of suramin and reactive blue 2 in preventing neuronal death induced by dequalinium. J Neurosci Res. 2000;62:692–9.
30. Chan CF, Lin-Shiau SY. Suramin prevents cerebellar granule cell-death induced by dequalinium. Neurochem Int. 2001;38:135–43.
31. Entelis NS, Kolesnikova OA, Martin RP, Tarassov IA. RNA delivery into mitochondria. Adv Drug Deliv Rev. 2001;49:199–215.
32. Entelis NS, Kolesnikova OA, Dogan S, Martin RP, Tarassov IA. 5 S rRNA and tRNA import into human mitochondria. Comparison of *in vitro* requirements. J Biol Chem. 2001;276:45642–53.
33. Entelis NS, Kieffer S, Kolesnikova OA, Martin RP, Tarassov IA. Structural requirements of tRNALys for its import into yeast mitochondria. Proc Natl Acad Sci USA. 1998;95:2838–43.
34. Kolesnikova O, Entelis N, Kazakova H, Brandina I, Martin RP, Tarassov I. Targeting of tRNA into yeast and human mitochondria: the role of anticodon nucleotides. Mitochondrion. 2002;2:95–107.
35. Koulintchenko M, Konstantinov Y, Dietrich A. Plant mitochondria actively import DNA via the permeability transition pore complex. EMBO J. 2003;22:1245–54.
36. Kajander OA, Rovio AT, Majamaa K, Poulton J, Spelbrink JN, Holt IJ, *et al.* Human mtDNA sublimons resemble rearranged mitochondrial genome found in pathological states. Hum Mol Genet. 2000;9:2821–35.